

Sedimentological Review of Upper Triassic (Mulussa F Formation) in Euphrates-Graben Syria

¹Ibrahim Yousef, ¹Vladimir Morozov and ²Mohammad Al-Kadi

¹Institute of Geology and Petroleum Technologies,
Kazan Federal University, Kazan, Russian Federation

²Department of Geology, Faculty of Science, Damascus University,
Damascus, Syrian Arab Republic

Abstract: Mulussa F formation is one of the important geological formations constituting the Mulussa group in Syria. The objective of this research is to review of sediments Mulussa F formation. Its deposits contain almost 50% of hydrocarbon potential through Euphrates Graben. Boreholes data permitted confining the formation between two Lithostratigraphic markers and enabled its division into three Lithostratigraphic members MUF3, MUF2, MUF1 (from bottom to top). Each member consists of a set of units, subunits and lithologic intervals. Petrology studying provides a precise petrological description of various formation members and their Diagenetic. Results show that the members of the structure are composed of continental detrital sediments made up of clay stones (Kaolinite/Illite) and Shale/Dolomitic clay stone, covered by intervals of quartz sandstones, clay sandstones and silt sandstones. The carbonate sediments are absent from the formation unless it's base which consists of Dolomitic clay stone and its top which are close to carbonate composition. This sediment of those members spread out as repeated or harmonic alternations whose faces gradients reflect transgression and regression sequences. Due to the historical value of Mulussa F formation, it is vital to investigate its sediments status. The study of these sediments leads to represent narrow barriers near river mouth with meandering channels and limited coastal deposits.

Key words: Euphrates Graben, Triassic, Mulussa F, stratigraphy, sedimentology, chemostratigraphy

INTRODUCTION

In Syria, three Mesozoic basins distinguished: the Palmyrides Basin, the Euphrates Graben and Sinjar Trough (Fig. 1). The west to NW-trending Euphrates Graben extends approximately 160 km from the E-W Anah Graben in Iraq to the northeastern edge of the Palmyrides Fold Belt (Fig. 1). It is about 90 km wide and reaches a maximum depth of about 5 km to the Triassic section. This Graben is described as a fault-controlled basin which resulted from flexing of the northeastern margin of the Arabian Plate, before abductions of the Tethyan oceanic crust during the late cretaceous.

MATERIALS AND METHODS

Study area: The study area covers Euphrates Graben, Syria (Fig. 2) with Mulussa F formation due to the special significance of its deposits at Euphrates Graben.

Geological setting: The 160 km long, Euphrates Graben (Fig. 1 and 2) system is interpreted as an aborted

Northwest trending intercontinental rift of Late Cretaceous age. It consists of a system of normal and strike-slip faults and is a result of a transdimensional regime (Fig. 3 and 4). Stratigraphy of the Euphrates Graben can be subdivided into three major Sequences: Pre-rift, Syn-rift and Post-rift Sequence.

RESULTS AND DISCUSSION

Description of the Mulussa F Formation: The Mulussa F formation is approximately 450 m thick (Fig. 5 and 6). Where igneous sills intrude, the thickness can increase up to 550 m. The formation consists mainly of floodplain Claystones interbedded with mostly medium-grained fluvial sandstones. Lagoonal and shallow-marine Dolomitic shales and dolomites are present in the lower part of the formation.

The Mulussa F formation is deposited conformably on top of the Mulussa E formation. The contact is gradational and no sedimentation break is suggested. Different formations cap the Mulussa F formation

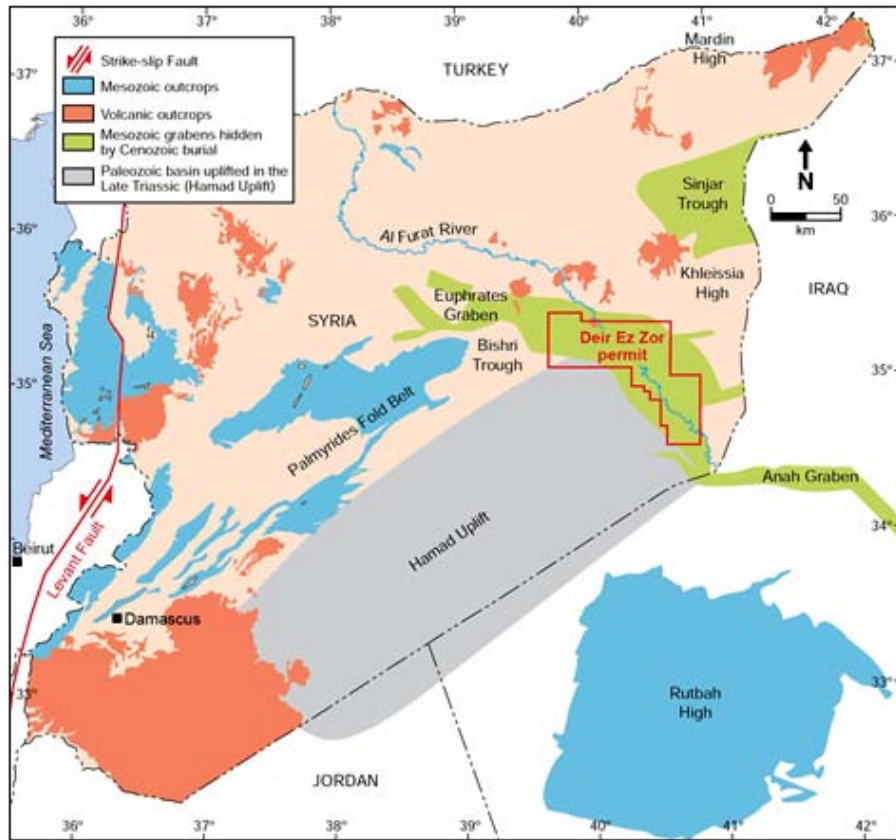


Fig. 1: Geological setting of Syria (Caron *et al.*, 2007)

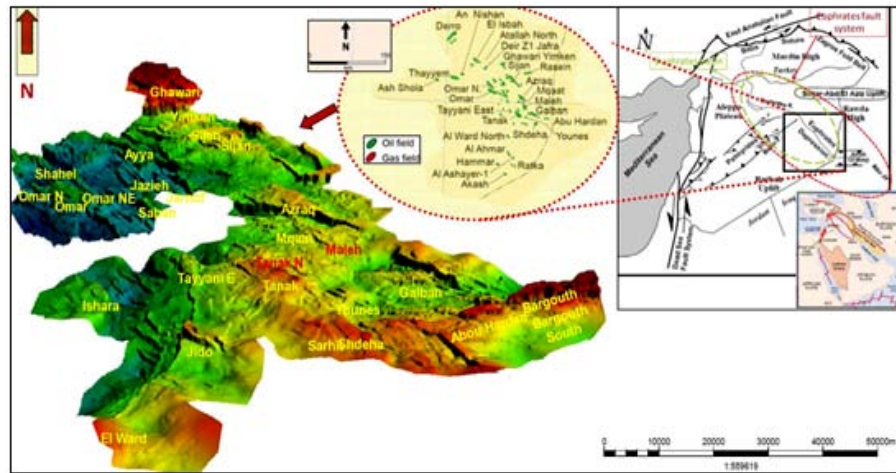


Fig. 2: Schematic of study area

depending on its position about the two major unconformity complexes, the BKL (Base Lower Cretaceous unconformity) and BKU (Base Upper Cretaceous unconformity) Fig. 7 (Litak *et al.*, 1997; Odedede and Adaikepoh, 2011) Palynological data suggests that the formatio has a Late Triassic

(Ladinian to Norian) age (Anari *et al.*, 2015; Ziegler, 2001) (Fig. 8). The formation is subdivided, by the Spectral Gamma Ray Logs, into three primary members Fig. 8: F3, F2 and F1. These members were divided further into subunits based on the lithology and N/G ratios (Fig. 8).

Petrology of the Mulussa F formation

Mulussa F3.2: The Mulussa F3.2 (Late Ladinian-Early Carnian) Fig. 8, unit is around 70 m thick. The unit consists of laminated and dark-grey Dolomitic Claystones with light gray dolomites interbedded (Plat: A). This unit is the most marine unit amongst the three with clear Palynological indications of marine influence. The Mulussa F3.2 is deposited conformably on top of the marine Dolomites of Mulussa E formation. The lower (seismic marker E) and upper (Dolomitic Marker DM) boundaries are gradual with no sedimentation gap (Fig. 8). The spectral gamma ray tool shows relatively low levels of Thorium and uranium with low-medium Potassium values increasing towards the top of unit (Fig. 9).

Mulussa F3.1: The unit is 57m thick; the thickness can increase up to 75 m where igneous sills intrude. This unit subdivided into a lower 'b' and an upper 'a' unit (Fig. 8). The basal 20 m of this unit (b) (Early Carnian) consists of Clayton's high content of Potassium with occasional 4-8 m sands at the top. The lowermost Claystones are laminated and dark-grey, similar to those of the Mulussa F3.2. These are overlain by olive-green de-stratified shales (Plat: A). The spectral gamma ray tool shows, relatively low levels of Thorium and Uranium and high levels of Potassium (Fig. 10). XRD analysis shows 40-70% of Illite dominated by Kaolinite (Plat XRD- I: 1, 2) and Fig.10. The upper 30 m of this unit (a) (Early to Middle Carnian) consists mainly of olive-green-reddish brown Claystone (Plat: B) with interbedded sandstones, 5-10 m thick. The Claystone are usually de-stratified.

Chemostratigraphical analysis Fig. 8 shows that the Potassium log of the NGT tool closely mimics the

measured K values with two low-K clay intervals in the top part of the unit, they correspond to two evolved soil horizons of light-purple color. XRD analysis on the K-lean intervals has shown that consists of 90% Kaolinite (Plat XRD- I: 3, 4) and Fig. 9 while the K-rich background shows a mixture of Illite and Kaolinite dominated by Kaolinite. The spectral gamma ray tool shows relatively high levels of Thorium and Potassium and a distinct increase in uranium (Fig. 11).

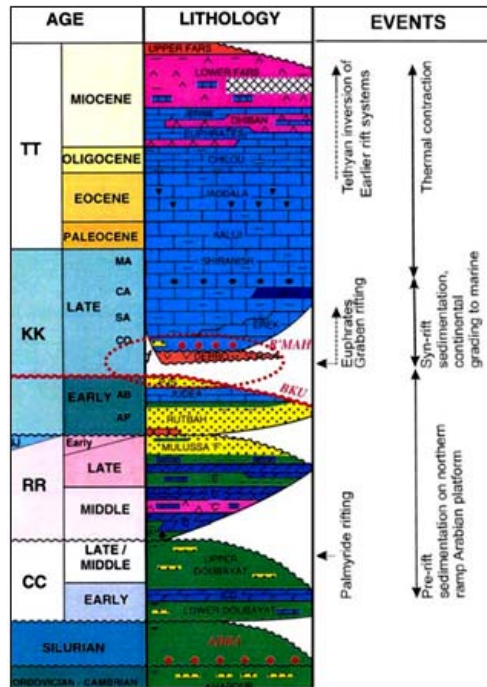


Fig. 3: General stratigraphy of the Euphrates Graben

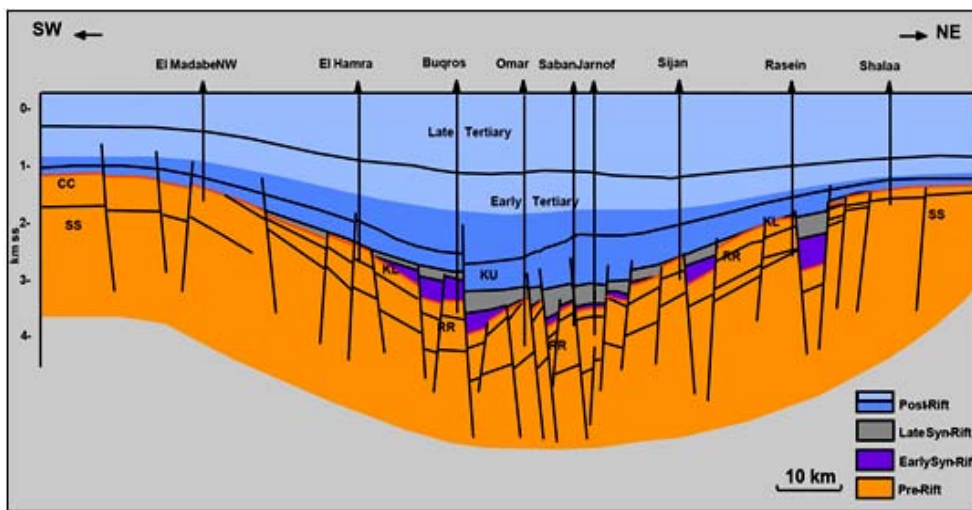


Fig. 4: Regional section across the Central Euphrates Graben from SW to NE

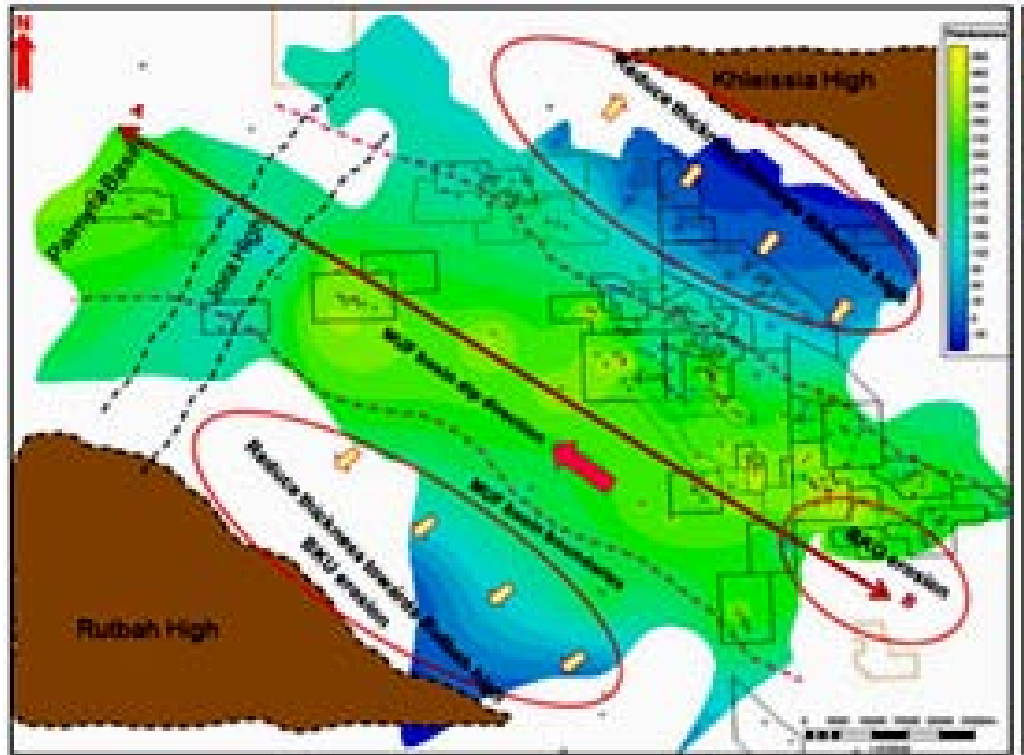


Fig. 5: Thickness map of Mulussa F formation in Euphrates Graben

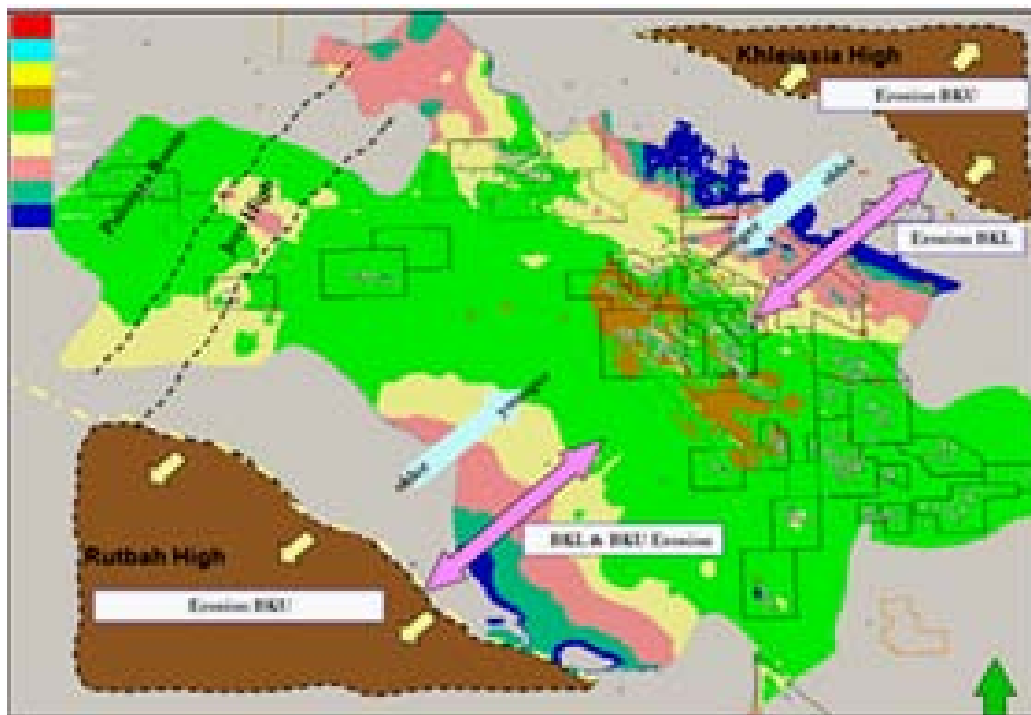


Fig. 6: Distribution map of Mulussa F lithostratigraphic units

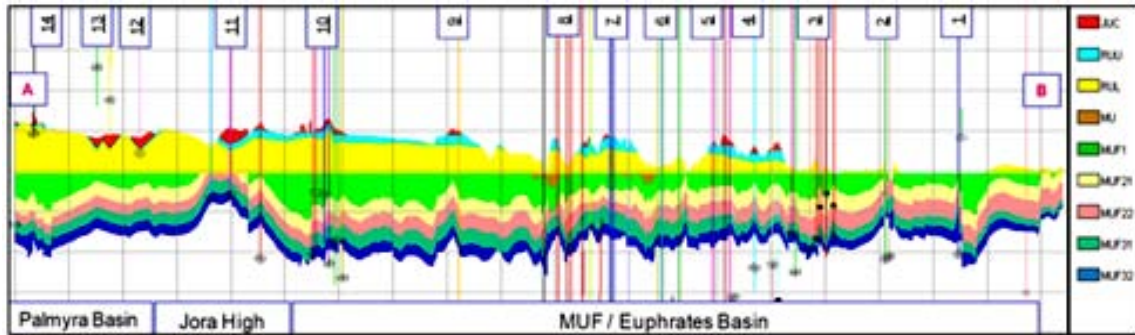


Fig. 7: Cross section A-B along Euphrates Grab

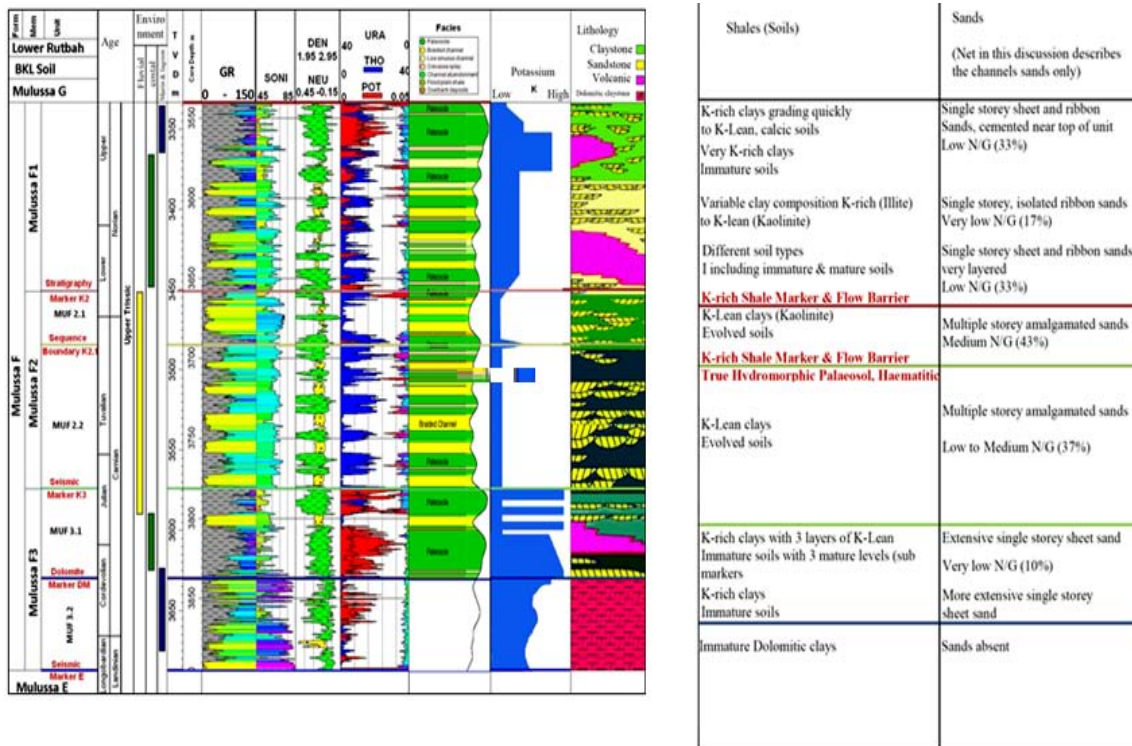


Fig. 8: Petrology of the Mulussa F formation

Mulussa F2.2: The Mulussa F2.2 Unit (Middle Carnian) is around 90 m thick. The unit consists mainly of pale-buff and light-grey Claystones with interbedded sandstones. The claystone show in places purple hues (Plat: C). This unit is the first one to be deposited in a clearly continental (fluvial) environment. The Mulussa F2.2 is deposited conformably on top of Mulussa F3.1. Figure 8 this unit is overlain by the floodplain clays of the Mulussa F2.1 Unit. The upper boundary is sharp (sometimes erosive) with clear evidence of a field wide sedimentation gap.

Chemostratigraphical analysis Fig. 8, on the clays, shows that in most of the Potassium originally contained

has been weathered, leaving a succession of veiny K poor clay intervals. XRD analysis indicates that the clays consist mainly of Kaolinite (Plat: II, 1, 2). The spectral gamma ray tool shows, for the shale intervals, relatively high levels of Thorium, very low level of Potassium and a variable uranium content profile.

Mulussa F2.1: The Mulussa F2.1 Unit (Late Carnian or Early Norian) is around 90 m thick. The unit consists mainly of pale-buff and light-grey claystone with interbedded sandstones. The claystone show in places marble-like gray patterns (Plat: D). The Mulussa F2.1 is

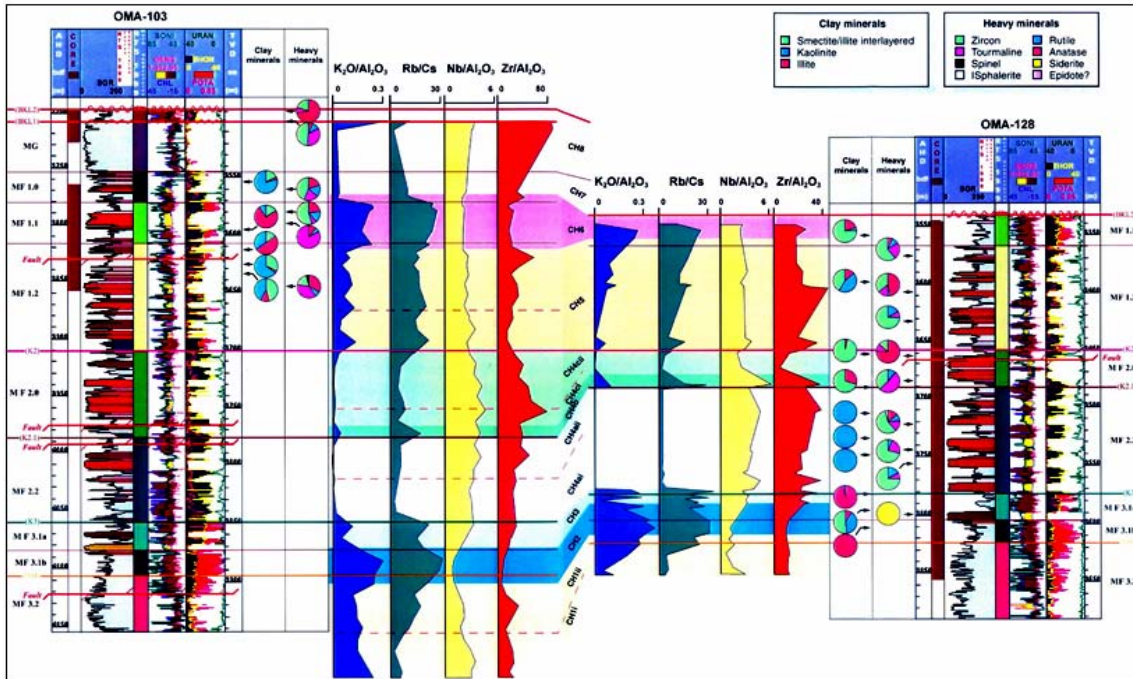


Fig. 9: Chemostratigraphical analysis of Mulussa F formation

deposited conformably on top of the Mulussa F2.2 Unit. This unit is overlain conformably by the floodplain clays of Mulussa F1.2 Unit. The upper boundary is called K2 Marker defined as the base of a high Potassium peak corresponding to the first K-rich (illicit) claystone bed after the long K-poor (Kaolinitic) section of the Mulussa F2 member (Fig. 8). Although, this marker is very clear on the Potassium log.

Chemostratigraphical analysis Fig. 8 (Ref. 22) on the clays shows that most of the Potassium originally contained has been weathered, leaving a succession of very K-poor clay intervals. XRD analysis (Plat XRD- II: 5, 6) and Fig. 9 indicates that the clays consist mainly of Kaolinite with some chlorite. The spectral gamma ray tool Fig. 12 shows, for the shale intervals, relatively high levels of Thorium, very low level of Potassium and a variable Uranium content profile.

Mulussa F1: The Mulussa F1 member is totally around 150 m thick. Where igneous sills intrude, the thickness can increase up to 200 m. The expected age of Mulussa F1 is (latest Early to Middle Norian). The Mulussa F1 member is subdivided into three units; the basal unit is Mulussa F1.2, the middle Mulussa F1.1 and the upper one Mulussa F1.0. The whole member consists mainly of Claystones of variable type and color (from light-med gray to brown-red) (Plat: E) with interbedded sandstones.

The Mulussa F1 is deposited conformably on top of Mulussa F2.0 Unit. The base is formed by a 5-15 m thick K-rich (Illicit) clay stone bed (Fig. 8). Also, the boundaries between the MUF1.2, MUF1.1 and MUF1.0 units are gradual with no evidence of a sedimentation gap Fig. 8.

Depending on how deep the BKL and BKU unconformity complexes erode, any of Mulussa F1 units, could be the youngest Triassic unit preserved. Where erosion does not reach the Mulussa F1, it is overlain by the carbonates of Mulussa G formation. This boundary is based on a sharp decrease in Thorium, Potassium, Gamma Ray and increase in density (Fig. 11).

The clays of MUF1.2: It shows, a very variable geochemical composition with a Potassium content ranging from low to medium and sometimes high (Fig. 8).

The XRD analysis (Plat XRD- III: 7) and Fig. 9 indicates that these clays are ranging from 75% Kaolinite (12% Illite, 9% Illite/Smectite, 4% chlorite) to 28% Kaolinite (34% Illite, 38% Illite/Smectite, 1% chlorite). The spectral gamma ray tool shows relatively high levels of Thorium, variable but usually very high, the level of Potassium and a variable Uranium profile.

The clays of MUF1.1: It shows an increase in Potassium Fig. 8. XRD analysis shows a composition dominated by Illite and Illite/Smectite and minor Kaolinite (up to 20%)

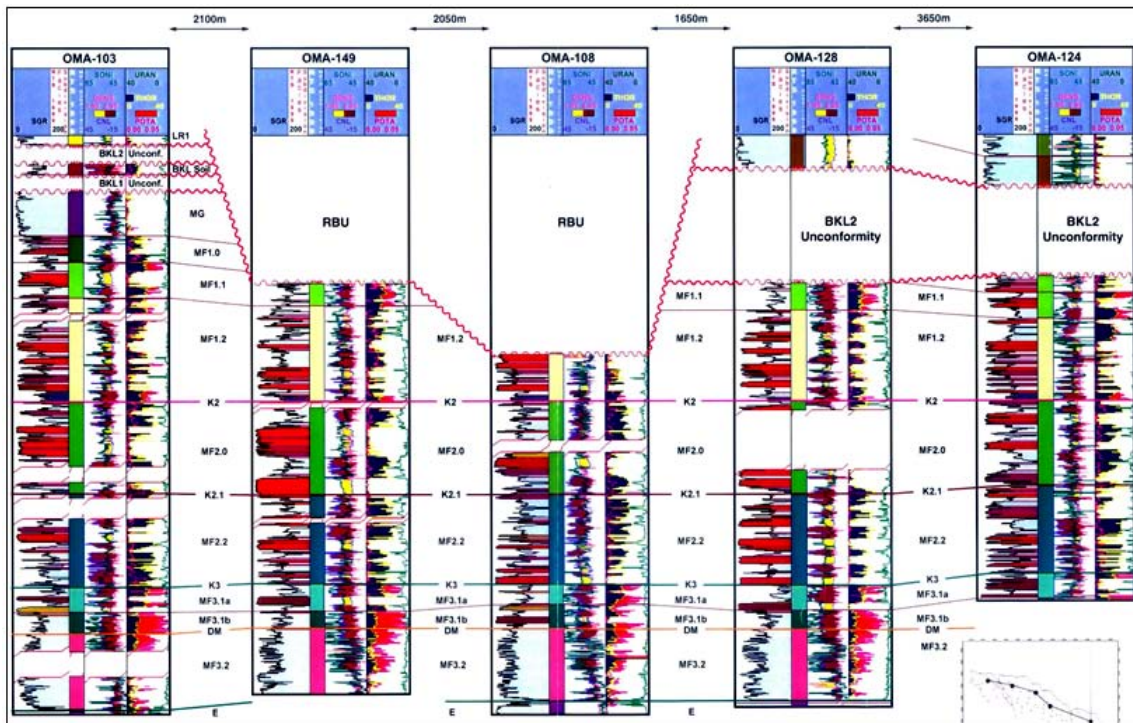


Fig. 10: Correlation panel of Mulussa F formation

(Plat XRD-III: 8) and Fig. 9, spectral gamma ray tool shows relatively high levels of Thorium, variable but usually the medium level of Potassium and a variable Uranium profile (Fig. 9).

The clays of MUF1.0: It shows a sharp decrease in Potassium (Fig. 8), XRD analysis shows a composition dominated by Kaolinite (75%) (Plat XRD-III: 9) and (Fig. 9). The spectral gamma ray tool shows, relatively lower levels of Thorium than in the rest of the Mulussa F, low to the very low level of Potassium and a variable Uranium profile (Fig. 13).

Mulussa F sandstone description: Sandstone intervals thin (0.6 m) and thick (11 m) are interbedded with the clays of Mulussa F. Four types of sandstone have been described (Plat: F, 9-12) (Miall, 1996, 2010).

Channel type A sands (category A facies): (Plat F: 1, 2) are medium-grained well sorted sands with cross-bedding. Often amalgamated. Such sandstones are believed to be part of a channel complex which was deposited, after erosion of the pre-existing clays under stable conditions.

Channel type B sands (category B facies): (Plat F: 3, 4, 5) are variable in Grain size, moderately to poorly sorted sands with cross-bedding (Fig. 12). Sandstones of this

type are rarely amalgamated and are interpreted as ephemeral channel deposits, possibly related to crevasse channel deposits (Barazangi *et al.*, 1993; Chaimov *et al.*, 1990).

Splay (Category C facies): (Plat F: 6, 7, 8) are fine-grained, shaly laminated sands with usually gradual contacts. These sands are usually thin and not amalgamated and probably represents splay and levee deposits.

Mouth bar fine sands (category B facies): (Plat F: 9-14) Are coarsening upward units with low-angle cross-stratification (Fig. 14 and 15). These intervals possibly represent small mouth bars deposited in shallow floodplain lakes by small deltas of crevasse channels. The Microscope Study (Plat: G) indicated that sandstone composed of Quartz Arenite⁷ to Quartz Wake⁸. In some intervals shows Kaolinitic Quartz Arenite⁹. The Quartz medium sorted, sub rounded to sub angular with size 250 to 500μm with cracked surfaces and worn edges. The grains are compacted together with semi-flat or concavo-convex contacts surfaces. In some points grains are connected with secondary radial syntaxial quartz which resulting from dissolution and quartz growth around clastic grains edges or in the open pores 10 looks as prismatic euhedral crystals its dimensions

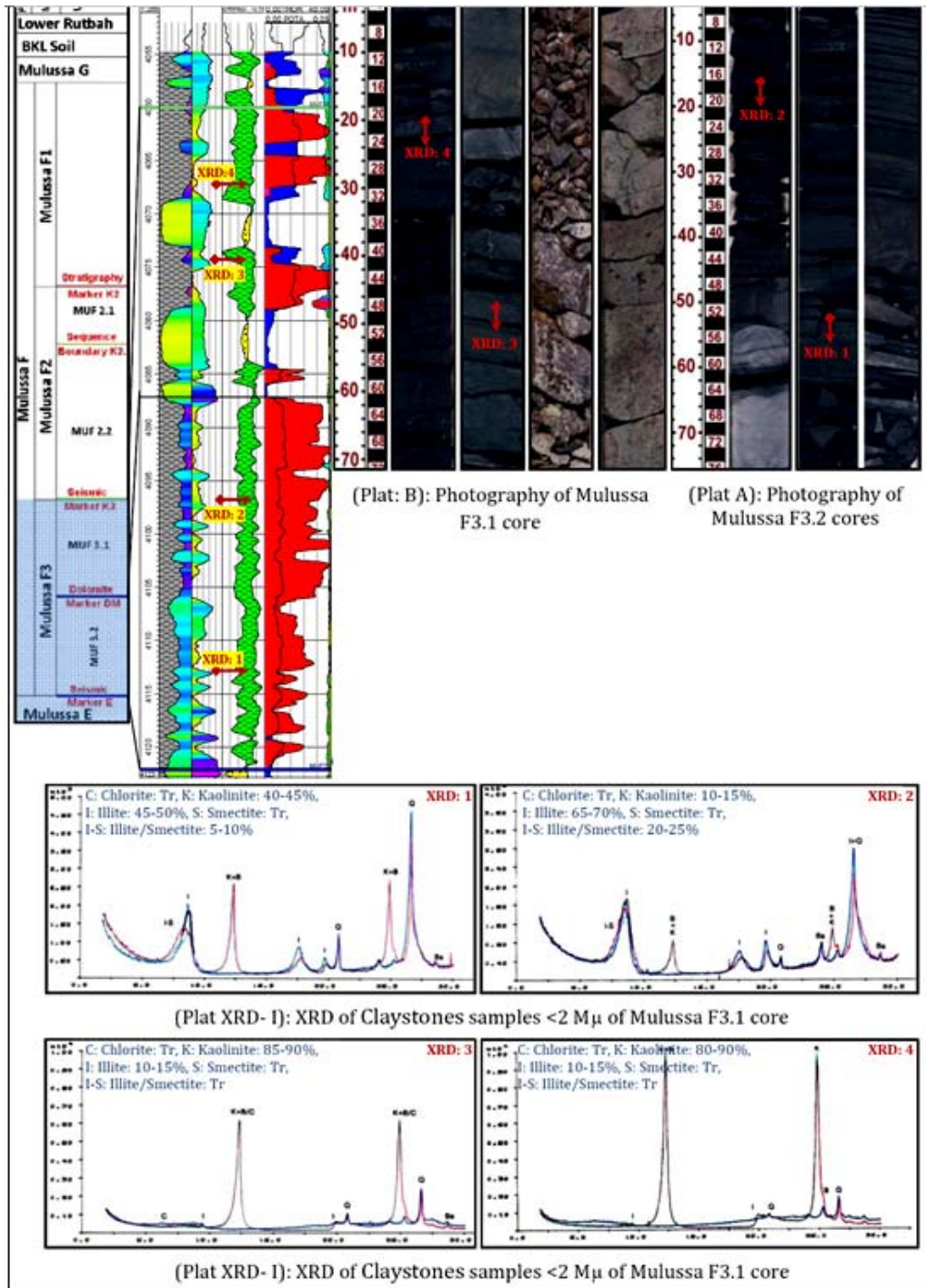


Fig. 11: Relatively high levels of Thorium and Potassium and a distinct increase in uranium

<50-100 M μ . This Syntaxial quartz cement in some cases looks overgrowth in pores network or around the grains or on its surfaces.

The components of this sandstone facies seem in some intervals are cemented hematite cement which forms

a thin arc edges around the grains and fills partly with Kaolinite. Also, its linings the pores walls and forms a Haematite linings and sometimes seem to be surrounded by the developing quartz So explain that forming of developing quartz later to form hematite (Fig. 16).

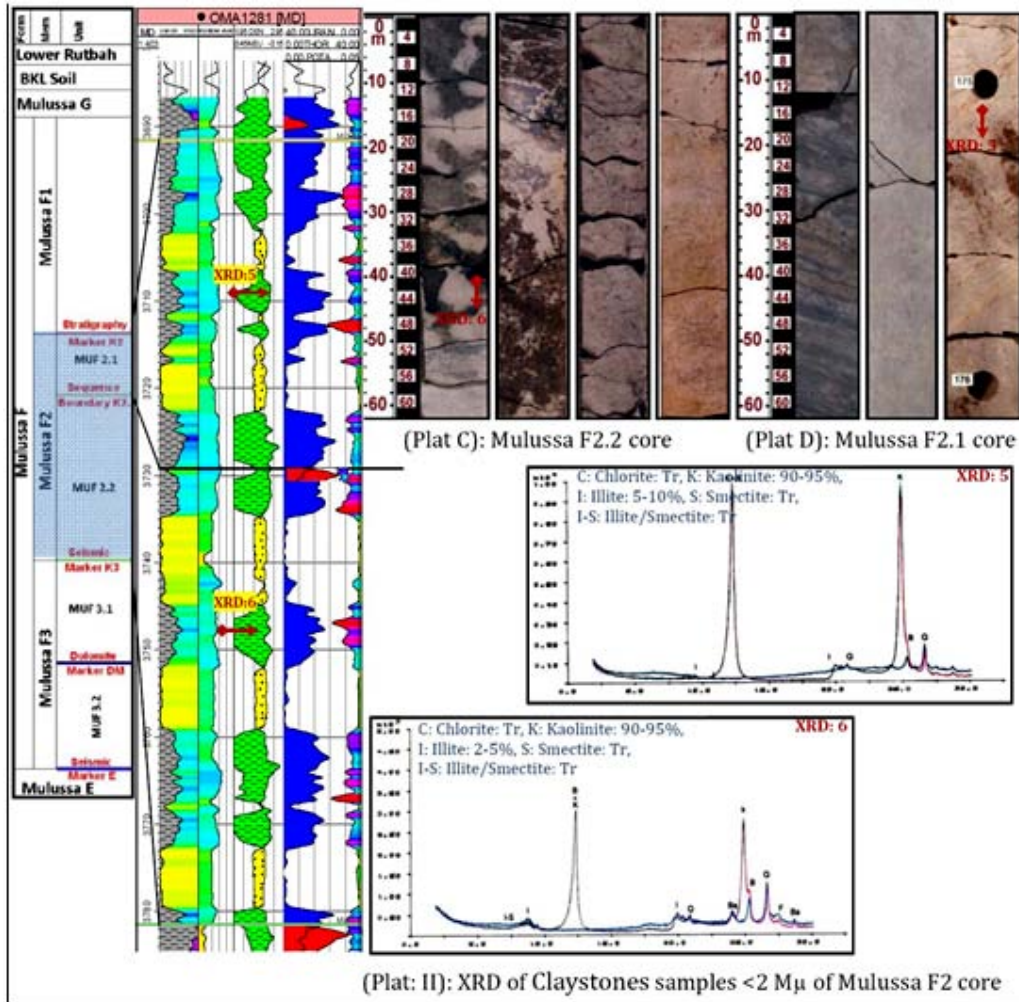


Fig. 12: Relatively high levels of Thorium, very low level of Potassium and a variable Uranium content profile

The first type crystals looks are big, flat and hierarchy of late stage, ranging between 50-150 M μ developing within the pore spaces and clog their throats (Hawie *et al.*, 2013; Caron and Mouty, 2007).

The second type looks the crystals are smaller, 40- 60 M μ and euhedral platelets tangled inclosing grains surfaces and retard its subsequent growth. Some Authigenic quartz crystals seem in the form of Saw-Tooth Overgrowths with dimensions 20-150 M μ as cement connects the detrital grains or look developing around the early Kaolinite crystals and partly enclosing it.

This facies of sandstone are mixed with 5-20% of detrital claystone, looks as cement between grains or as spots/patches of matrix constitute of thin-weak growth platelets of Illite/Smectite within the pores network. This claystone sometimes looks consisting of Euhedral; Pseudo-Hexagonal and Rhombohedral platelet

of Kaolinite up to 20 M μ arranged within pores network as vermicular or blocky Kaolinite replaces the detrital clay (Sawaf *et al.*, 1993).

Detrital Claystones lesser seems composed of early chlorite origination and usually happens as a stage of packaging/enclosing and replace detrital grains or as flat crystals up to 15 M μ filling the pores and blocked/enclosed by Authigenic quartz. This chlorite claystone sometimes seems as crystals and platelets with late genesis and smaller and less crystallized and ensure vertically or randomly on the grains surface and hinder its growth or intertwined to form clusters within the pores network and form a microscopic porosity between the crystals retain grains frames (Harold, 1996).

The sediment of this facie also mixed with the Siderite (1-23%) which founded as clusters concentrated in pores

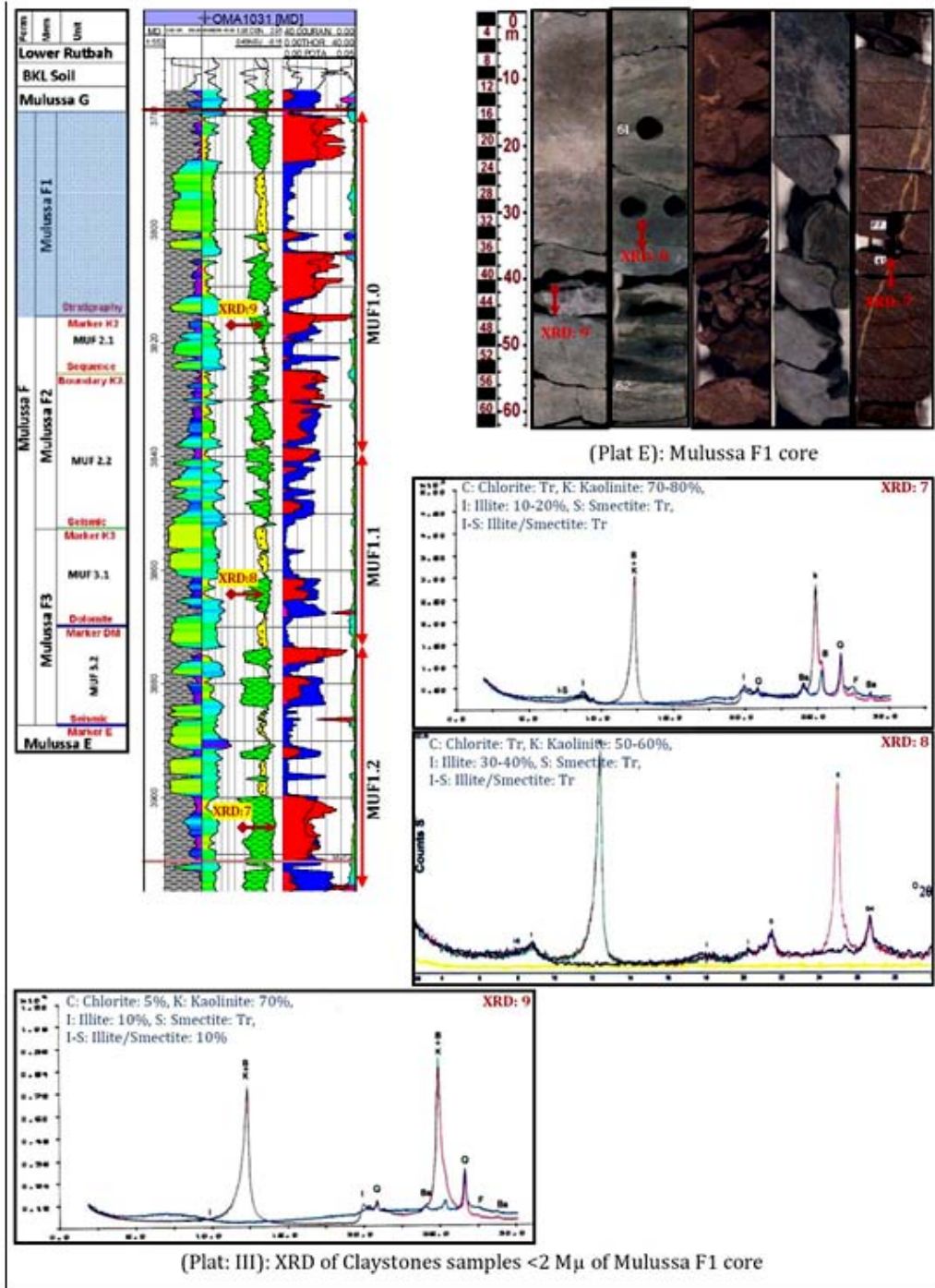


Fig. 13: Relatively lower levels of Thorium than in the rest of the Mulussa F, low to very low level of Potassium and a variable Uranium profile

network of ranging in size from a few microns to 150 M μ and leads collected to form Sphaerosiderite size of <2.3 mm concentrated around zones rich roots.

Siderite also can be found as Poikilotopic cement or in the form of Subhedral crystals in pores network or as nodules.

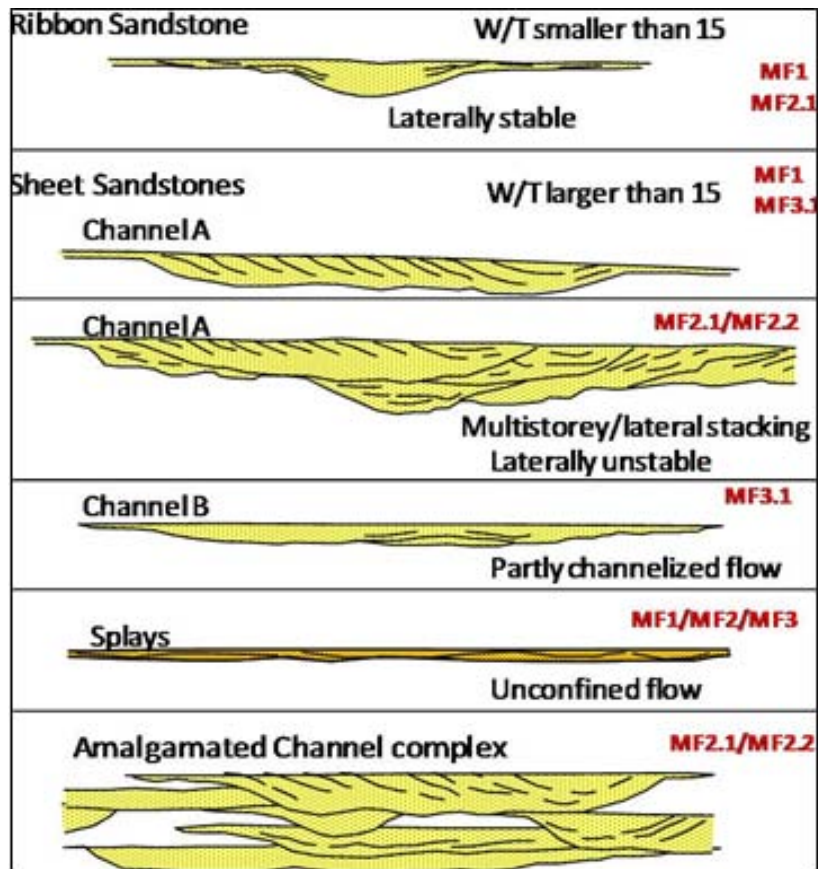


Fig. 14: Sandstone body classification (Miall, 1996)

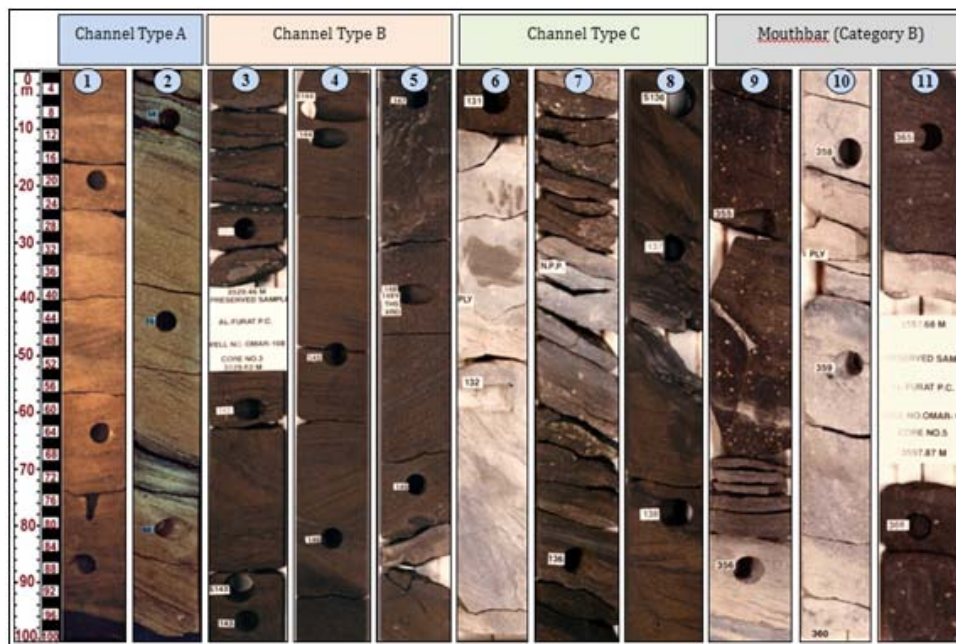


Fig. 15: (Plat F): Mulussa F sandstone core photographs

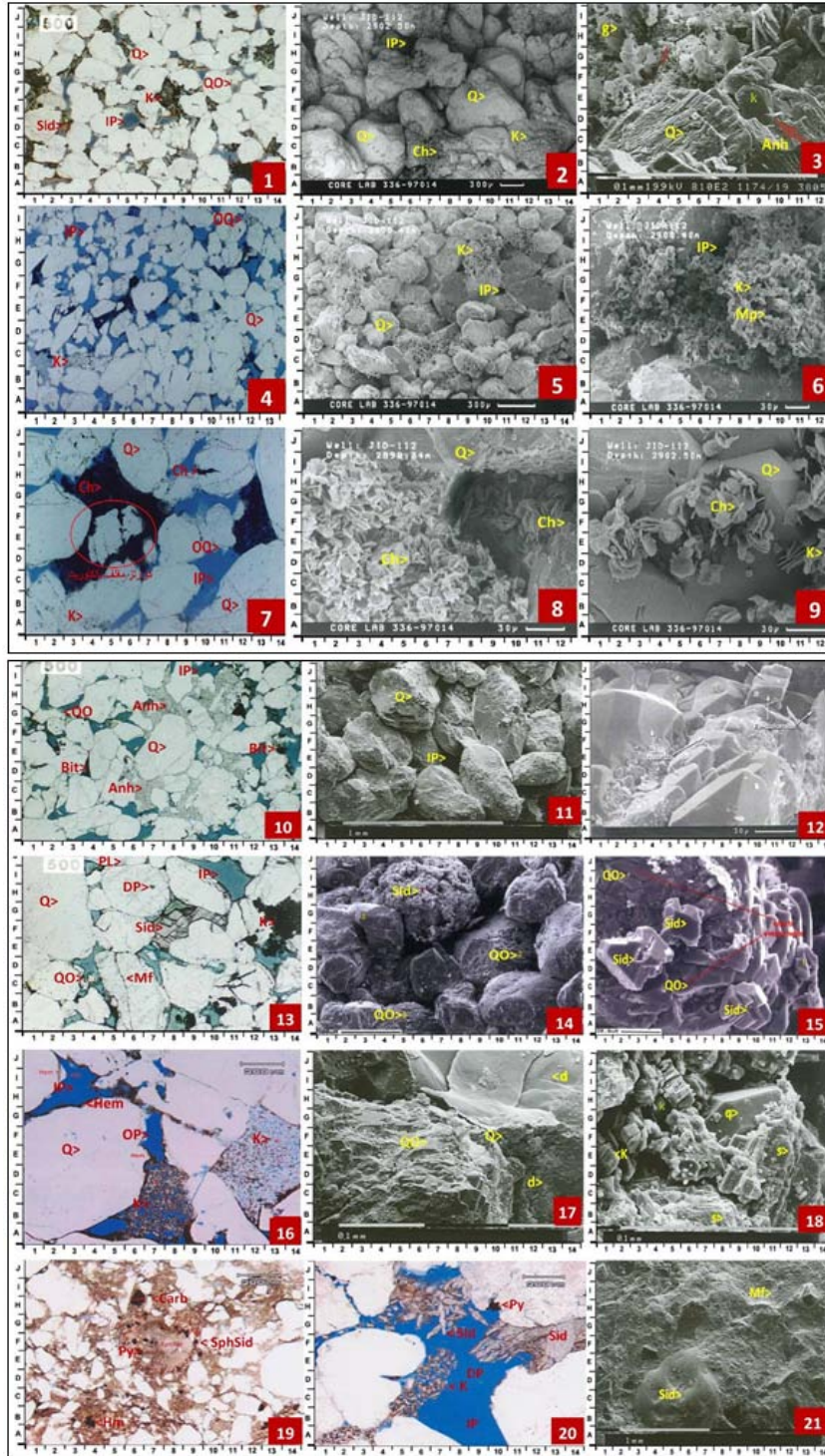


Fig. 16: (Plat G): Polarized/electron microscope slides photos of sandstone samples from Mulussa; QO: quartz over growth, Q: quartz, K: Kaolinite, Ch: chlorite, F: Feldspars, Zr: Zircon, To: Tourmaline, Py: Pyrite, Sid: Siderite, Anhy: Anhydrite, IP: Intergranular Porosity, Mp: Microscopic Porosity, Dp: Dissolution Porosity, PL: Planer Contacts, PT: Pore Throat, CC: Concave Convex Contacts, To: Titanium Oxide, SphSid: Siderite Nodules, Hem: Hematite, OP: Open Porosity Quartz overgrowth shows using electron microscope two types of Size/Age

CONCLUSION

The fluvialite Melissa F formation Late Triassic age is up to 450 m thick and is preserved only in the central part of the euphrates Graben system. The thickness of the formation is variable due to the erosion caused by BKL and BKU Complex in the area. The formation can be split into three members (Mulussa F3 to F1) separated by two major markers (K3 and K2) and eight units (Mulussa F3.2, F3.1b, F3.1a, F2.2, F2.1, F1.2, F1.1 and F1.0). The BKL unconformity and the K2.1 Marker separating the Mulussa F2.2 unit from the Mulussa F2.0 unit are regarded as Sequence Boundaries. It is probably that the K3 Marker represents a third Sequence Boundary in the succession (Fig. 8).

The Mulussa F formation records both a progradation, from the underlying Mulussa E formation to the K2.1 marker in the middle of Mulussa F2 member and a retrogradation from the K2.1 marker to overlying Mulussa G formation.

ACKNOWLEDGEMENT

The research is performed according to the Russian Government Program of Competitive Growth of Kazan Federal University.

REFERENCES

- Anari, M., N.K. Ghadimvand, A. Kangazian and S.H. Hejazi, 2015. Facies analysis, sedimentary environment and sequence stratigraphy of the lower cretaceous deposits in the Kalahroud Area, at North of Esfahan, Iran. *Indian J. Sci. Technol.*, 8: 1-9.
- Barazangi, M., D. Seber, T. Chaimov, J. Best and R. Litak *et al.*, 1993. Tectonic Evolution of the Northern Arabian Plate in Western Syria. In: *Recent Evolution and Seismicity of the Mediterranean Region*, Boschi, E., E. Mantovani and A. Morelli (Eds.). Springer, Netherlands, ISBN:978-94-010-4891-0, pp: 117-140.
- Caron, C. and M. Mouty, 2007. Key elements to clarify the 110 million year hiatus in the Mesozoic of Eastern Syria. *Geo Arabia*, 12: 15-36.
- Chaimov, T.A., M. Barazangi, A.D. Saad, T. Sawaf and A. Gebran, 1990. Crustal shortening in the Palmyride fold belt, Syria and implications for movement along the Dead Sea fault system. *Tectonics*, 9: 1369-1386.
- Harold, G., 1996. *Reading Sedimentary Environments: Processes, Facies and Stratigraphy*. 3rd Edn., Wiley-Blackwell, Australia.
- Hawie, N., D. Granjeo and C. Muller, 2013. Sedimentological and stratigraphic evolution of northern Lebanon since the late cretaceous: Implications for the Levant margin and Basin. *Arabian J. Geosci.*, 7: 1-27.
- Litak, R.K., M. Barazangi, W. Beauchamp, D. Seber and G. Brew *et al.*, 1997. Mesozoic-Cenozoic evolution of the intraplate Euphrates fault system, Syria: Implications for regional tectonics. *J. Geol. Soc.*, 154: 653-666.
- Miall, A., 2010. *The Geology of Stratigraphic Sequences*. Springer, Berlin, Germany, Pages: 522.
- Miall, A.D., 1996. *The Geology of Fluvial Deposits: Sedimentary Facies, Basin Analysis and Petroleum Geology*. Springer, Berlin, Germany, ISBN-13: 9783540591863, Pages: 582.
- Odedede, O. and E.O. Adaikpoh, 2011. Sequence stratigraphic analysis of the Gombe sandstone and lower kerrickeri formation exposed around Fika-potiskum, Upper Benue Trough, Nigeria: A consideration for petroleum reservoir indicators. *Indian J. Sci. Technol.*, 4: 492-498.
- Sawaf, T., A.D. Saad, A. Gebran, M. Barazangi and J.A. Best *et al.*, 1993. Stratigraphy and structure of eastern Syria across the Euphrates depression. *Tectonophysics*, 220: 267-281.
- Ziegler, M.A., 2001. Late Permian to Holocene Paleofacies evolution of the f the Arabian plate and its hydrocarbon occurrences. *Gulf Petro Link Bahrain*, 6: 445-510.